

Effect of Shorting Wall on Compact 2×4 MSA Array Using Artificial Neural Network

Mohammad Aneesh^{*1}, Jamshed Aslam Ansari², Ashish Singh³, Km. Kamakshi⁴

Microwave Antenna Research Centre, Department of Electronics & Communication,
University of Allahabad, Allahabad – 211002, UP India

*Corresponding author, email: aneeshau14@gmail.com¹, jaansari@rediffmail.com²,
ashsin09@rediffmail.com³, kamakshi.kumar21@gmail.com⁴

Abstract

In this paper, a compact 2×4 microstrip antenna (MSA) array is presented and the effect of inserting shorting wall is optimized with the help of artificial neural network (ANN). An ANN model has been developed for predicting the resonant frequencies with the variation of the height of substrate and shorting wall position. For validation of ANN output, a prototype of 2×4 MSA array is physically fabricated and tested. This validation verifies the proposed antenna for which simulated and ANN results are approximately similar.

Keywords: microstrip antenna array, artificial neural network, multiband, shorting wall

Copyright © 2015 Institute of Advanced Engineering and Science. All rights reserved.

1. Introduction

Over last decade MSAs are well accommodated to wireless applications due to its distinguish features such as low profile structures, light weight, low cost, and easy fabrication of different radiating shapes [1]. There has been a lot of research on MSA in respect to different shapes. The shape of radiating patch plays a vital role to enhance the antenna characteristics. This led to produce lots of research work for different shapes of MSAs such as, W-shaped patch [2], E-shaped patch [3], half E-shaped patch [4], S-shape antenna [5], and gap coupled microstrip array antenna [6]. MSA arrays are widely used in many practical applications due to their planar structures and burning issue for research among the researchers in previous days. Several investigations have been done by researchers on MSA arrays such as, a single layer monopulse array [7], cylindrical array antenna [8], array using electromagnetic band gap (EBG) structures [9-10], and a 2×2 MSA array with microstrip line feed tooth-like-slot patches [11]. In addition, MSA array on an irregular dielectric surface and Teflon substrate are investigated [12-13]. Further, design and performance analysis of series feed and corporate feed MSA array have been carried out [14]. A spiral array for ultra wideband [15], filtering MSA array [16], and stacked patches for two dimensional planar array topologies [17] gained much attention of researchers. All the above reported papers are mainly based on the theoretical, simulation, and experimental results. Further to increase the credibility of results it has been subjected to ANN. As ANN provides fast and accurate modelling due to it has gained interest of researchers. The various applications of ANN have been utilized in the field of MSA arrays such as, fault finding [18], frequency modelling [19], the effect of microstrip feed line width on array [20], photonic band gap (PBG) structures on cylindrical MSA [21]. Several other techniques are also used for the design and analysis of MSA array [22-24] and they produce fast and accurate results. In [25], a 64-element array was proposed for Ka-band with rotation feeding technique.

This work has been inspired from above literature and dedicated to the design of a compact 2×4 MSA array whereas the effect of inserting shorting wall on the proposed antenna array is optimized with the help of ANN. Thereafter proposed antenna is fabricated and measured results are compared with ANN optimization and simulated results.

The rest of the paper is organized in the following manner; section 2 holds an overview of design and simulation of antenna array which also includes the generation of simulated data for ANN model. Then in section 3, results and discussion are elaborated for ANN study and fabricated proposed antenna. Finally in section 4, the conclusion of the overall study is drawn.

2. Design and Simulation of Antenna Array

This section shows the geometry formation process of proposed antenna array. Figure 1(a) shows, 2×4 array of patch antennas in which each patch is size of $L \times W$ on glass epoxy substrate ($h = 1.60\text{mm}$). All these patches are etched with L_g distance and interconnected with 50Ω microstrip lines of sizes $L_{SA} \times W_{SA}$, $L_{SB} \times W_{SB}$. The total area occupied by this patch geometry is $L_{FA} \times W_{FA} \times h$. Further, in Figure 1(b), a shorted wall is added in radiating patches (RP) one by one from RP1 to RP8. Multiband response is achieved by adding this shorting wall as shown in Figure 2. All the respective values regarding design specifications are summarized in Table 1. These antenna geometries are simulated in IE3D software [26]. The reflection coefficient variation with frequency for shorting wall positions at RP1 to RP8 is shown in Figure 3 and observed that there is no drastic change occurs in the value of resonating frequencies only the dip of the reflection coefficient is varied from -10 dB to -34 dB. Whereas the effect of inserting shorting wall on radiating patches is the main cause for its multiple frequency bands.

Table 1. Design specifications

Parameter	Value	Sample
L	6 mm	-
W	10 mm	-
L_g	1 mm	-
L_{FA}	27 mm	-
W_{FA}	27 mm	-
L_{SA}	7 mm	-
W_{SA}	1 mm	-
L_{SB}	22 mm	-
ϵ_r	4.7	-
h	1.60 mm	$1.57 \leq h \leq 1.60$
SWP	RP2	RP1 to RP8

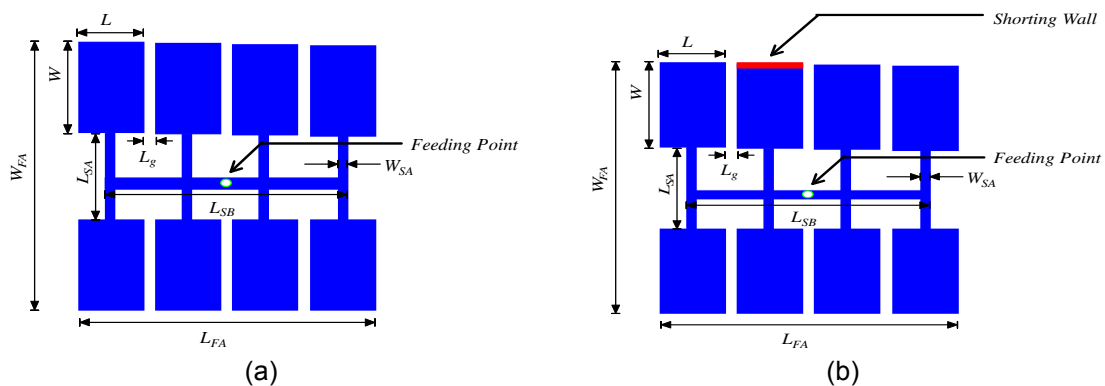


Figure 1. Simulated design of (a) 2×4 MSA array (b) 2×4 MSA array with shorted wall at RP2

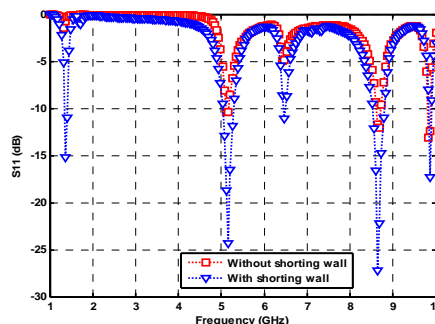


Figure 2. Reflection coefficient response of 2×4 MSA array with and without shorted wall

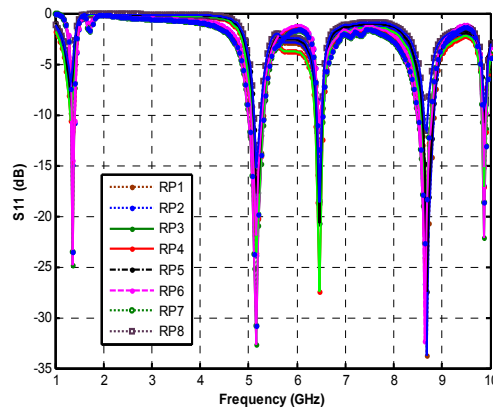


Figure 3. Variation in reflection coefficient with frequency for different shorting wall location

2.1. Data Generation from Simulated Results for ANN Model

This section describes about generation of data from IE3D simulator for ANN model’s training and testing. Here 32 antennas are generated in simulation media with a variety of shorting wall position from RP1 to RP8 and height of the substrate (h). The resonating frequencies (f_r) and radiation efficiencies (R_e) of these 32 simulated antennas are recorded and given in Table 2. These data samples are used for training and testing of ANN model.

Table 2. Simulated data for training and testing of ANN model

	SWP	ϵ_r	h	L_g	R_{e1}	R_{e2}	R_{e3}	R_{e4}	R_{e5}	f_{r1}	f_{r2}	f_{r3}	f_{r4}	f_{r5}
Training Data	1	4.7	1.57	1	0.675	0.874	0.714	0.835	0.703	1.31	5.25	6.34	8.26	9.54
	2	4.7	1.57	1	0.678	0.734	0.650	0.804	0.745	1.32	5.25	6.42	8.73	9.86
	3	4.7	1.57	1	0.574	0.716	0.623	0.810	0.711	1.31	5.32	6.45	8.47	9.70
	4	4.7	1.57	1	0.648	0.743	0.641	0.863	0.716	1.30	5.48	6.25	8.46	9.81
	5	4.7	1.57	1	0.678	0.754	0.648	0.843	0.730	1.29	5.67	6.43	8.71	9.24
	6	4.7	1.57	1	0.699	0.795	0.674	0.817	0.721	1.30	5.65	6.52	8.68	9.41
	7	4.7	1.57	1	0.725	0.841	0.645	0.837	0.719	1.35	5.45	6.79	8.64	9.74
	8	4.7	1.57	1	0.784	0.803	0.685	0.836	0.701	1.34	5.37	6.63	8.56	9.64
	1	4.7	1.58	1	0.642	0.802	0.768	0.812	0.754	1.25	5.61	6.30	8.40	9.90
	2	4.7	1.58	1	0.645	0.874	0.688	0.847	0.747	1.29	5.60	6.22	8.39	9.93
	3	4.7	1.58	1	0.654	0.897	0.623	0.865	0.753	1.28	5.75	6.25	8.27	9.94
	4	4.7	1.58	1	0.754	0.869	0.695	0.811	0.717	1.26	5.74	6.29	8.29	9.93
	5	4.7	1.58	1	0.786	0.874	0.684	0.842	0.702	1.22	5.64	6.28	8.37	9.92
	6	4.7	1.58	1	0.805	0.841	0.637	0.821	0.715	1.23	5.67	6.27	8.31	9.95
	7	4.7	1.58	1	0.745	0.861	0.694	0.823	0.734	1.27	5.81	6.21	8.28	9.91
	8	4.7	1.58	1	0.684	0.844	0.678	0.895	0.716	1.29	5.63	6.24	8.38	9.94
	1	4.7	1.59	1	0.824	0.874	0.687	0.841	0.736	1.20	5.83	6.23	8.26	9.95
	2	4.7	1.59	1	0.812	0.814	0.674	0.845	0.754	1.13	5.85	6.15	8.18	10.1
	3	4.7	1.59	1	0.838	0.848	0.669	0.841	0.745	1.18	5.91	6.18	8.13	9.97
	4	4.7	1.59	1	0.756	0.804	0.669	0.804	0.700	1.19	5.90	6.22	8.20	9.99
	5	4.7	1.59	1	0.778	0.831	0.678	0.845	0.718	1.16	5.86	6.20	8.22	9.98
	6	4.7	1.59	1	0.718	0.841	0.645	0.864	0.730	1.17	5.84	6.21	8.13	9.96
	7	4.7	1.59	1	0.641	0.867	0.654	0.884	0.732	1.15	5.88	6.17	8.24	9.95
	8	4.7	1.59	1	0.653	0.845	0.647	0.888	0.712	1.19	5.87	6.16	8.25	10.0
Testing Data	1	4.7	1.60	1	0.824	0.900	0.724	0.905	0.774	1.23	5.31	6.34	8.62	10.2
	2	4.7	1.60	1	0.812	0.905	0.735	0.919	0.780	1.25	5.25	6.42	8.73	9.86
	3	4.7	1.60	1	0.838	0.845	0.710	0.906	0.765	1.18	5.38	6.39	8.71	9.60
	4	4.7	1.60	1	0.756	0.854	0.707	0.910	0.710	1.11	5.45	6.21	8.66	9.75
	5	4.7	1.60	1	0.778	0.896	0.711	0.904	0.768	1.09	5.46	6.32	8.84	9.74
	6	4.7	1.60	1	0.718	0.886	0.720	0.898	0.745	1.08	5.42	6.43	8.88	9.63
	7	4.7	1.60	1	0.641	0.884	0.704	0.884	0.775	1.14	5.34	6.27	8.79	9.90
	8	4.7	1.60	1	0.653	0.890	0.718	0.914	0.740	1.07	5.39	6.48	8.64	9.98

2.2. ANN Model Selection for the Analysis of Proposed Antenna

ANN is a computational tool (model) which is inspired by biological nervous system and these networks uses several topologies. One of the most popular topology is the multilayer perceptron (MLP) neural network due to its supervised and unsupervised learning strategies. So this is the leading reason for adapting MLP-ANN in this work. MLP is a feed forward neural network and comprises many neurons in input, output and hidden layers. Each layer plays a different role in ANN model. In this work, three layered MLP-ANN model of structure 9×60×5 is selected. It means this model comprises 9 neurons in input layer, 60 neurons in hidden layer and 5 neurons in the output layer as shown in Figure 4. The other parameters are selected as, learning rate (η) = 0.001, momentum coefficient (μ) = 0.75, error goal (eg) = 0.00001, and $MSE = 1.21 \times 10^{-5}$. This MLP model is trained with Levenberg Marquardt algorithm [27] whereas weights and biases are updated between 0 and 1. Twenty eight data sets from Table 2 are used for the training of ANN model, and remaining eight data sets are used for testing of ANN model. In this model simulated data pattern, shorting wall position (SWP), ε_r , h , L_g , R_{e1} , R_{e2} , R_{e3} , R_{e4} , and R_{e5} are used as input and their respective resonating frequencies f_{r1} , f_{r2} , f_{r3} , f_{r4} , and f_{r5} are considered as output for this model. Then, during the testing of ANN model, mean square errors (MSE) between the simulated and ANN results are computed as [28]:

$$MSE = \frac{1}{n} \sum_{i=1}^n [x_i - f_{ANN}(y_i)]^2 \quad (1)$$

Where x_i is the final output of ANN model and calculated as:

$$x_i = f_2[w^2](f_1[w^1][y_i] + [b^1])) + [b^2]) \quad (2)$$

Where y_i is the input function matrix and given as:

$$[y_i] = [SWP \quad \varepsilon_r \quad h \quad L_g \quad R_{e1} \quad R_{e2} \quad R_{e3} \quad R_{e4} \quad R_{e5}]^T \quad (3)$$

Where w^1 and w^2 are the weight matrices of hidden and output layer and given as:

$$[W^1] = \begin{bmatrix} W^1_{1,1} & W^1_{1,2} & \dots & W^1_{1,9} \\ W^1_{2,1} & W^1_{2,2} & \dots & W^1_{2,9} \\ \cdot & \cdot & \dots & \cdot \\ \cdot & \cdot & \dots & \cdot \\ W^1_{60,1} & W^1_{60,2} & \dots & W^1_{60,9} \end{bmatrix} \quad (4)$$

$$[W^2] = \begin{bmatrix} w^2_{1,1} & \dots & w^2_{1,5} \\ \cdot & \dots & \cdot \\ W^2_{30,1} & \dots & W^2_{30,5} \end{bmatrix} \quad (5)$$

Where b^1 and b^2 are the bias matrices for hidden and output layer and given as:

$$[b^1] = [b^1_1 \quad b^1_2 \quad \dots \quad b^1_{60}]^T \quad (6)$$

$$[b^2] = [b^2_1 \quad b^2_2 \quad \dots \quad b^2_5]^T \quad (7)$$

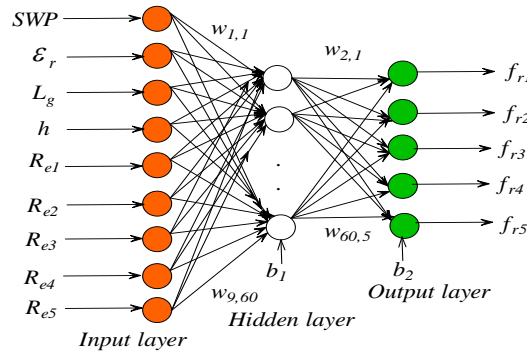


Figure 4. MLP-ANN model

3. Results and Analysis

This section elaborates the experimental results of the proposed method which provides a separate analysis of ANN optimization and validation study.

3.1. ANN Results

In the training of ANN model, simulated data patterns are used as input and output functions, as previously discussed. After the proper training, ANN model is subjected to testing for IE3D generated data for shorted wall 2x4 MSA array. Testing data sets are selected for substrate height (h) = 1.60 mm and shorted wall position from $RP1$ to $RP8$ as tabulated in Table 2. MLP-ANN model predicted the approximately similar results for resonant frequencies and these results are compared with the IE3D simulated results as given in Table 3. One of the tested data set is physically fabricated and measured for validation of this work and given in the next section. The fabricated data set has been highlighted in the Table 2 and Table 3. Figure 5 shows the comparison between simulated and ANN optimized frequencies for different test patterns.

Table 3. Comparison of IE3D, ANN results

IE3D Simulated (Target)					ANN output				
f_{r1}	f_{r2}	f_{r3}	f_{r4}	f_{r5}	f_{r1}	f_{r2}	f_{r3}	f_{r4}	f_{r5}
1.23	5.31	6.34	8.62	10.2	1.203	5.312	6.314	8.612	10.202
1.25	5.25	6.42	8.73	9.86	1.253	5.252	6.425	8.734	9.866
1.18	5.38	6.39	8.71	9.60	1.184	5.378	6.389	8.713	9.602
1.11	5.45	6.21	8.66	9.75	1.101	5.445	6.213	8.664	9.745
1.09	5.46	6.32	8.84	9.74	1.092	5.464	6.326	8.854	9.734
1.08	5.42	6.43	8.88	9.63	1.087	5.425	6.437	8.878	9.634
1.14	5.34	6.27	8.79	9.90	1.140	5.334	6.274	8.794	9.907
1.07	5.39	6.48	8.64	9.98	1.073	5.389	6.488	8.634	9.989

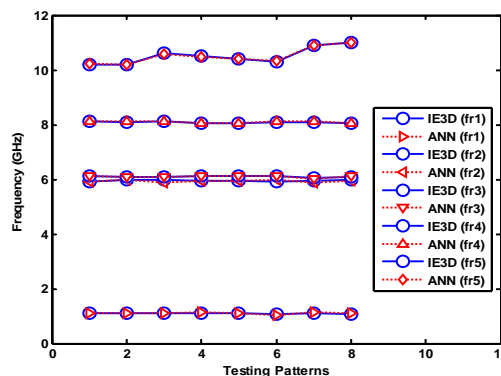


Figure 5. Comparison of simulated and ANN frequencies

3.2. Validation of ANN Study

For the validation of ANN study a prototype of 2×4 microstrip antenna array with a shorted wall at RP2 is physically fabricated on glass epoxy ($\epsilon_r = 4.7$) substrate as shown in Figure 6(a). An SMA connector of 0-18 GHz is used here for the excitation of geometry. The reflection coefficient and radiation pattern of fabricated geometry are measured in Agilent N5230A network analyzer and an anechoic chamber respectively for proving of ANN results.

Figure 7 shows the comparison between simulated and measured reflection coefficient ($S_{11} \leq -10\text{dB}$) for 2×4 MSA array with a shorted wall at RP2. The figure reveals that the fabricated antenna operates at multiple frequency bands of 1.32, 5.25, 6.42, 8.73, 9.86 GHz, which is useful for L, C, and X band applications. Simulated and measured results are in close agreement; only minor divergence takes place in measured value of S_{11} due to the oddity in fabrication and losses which are not considered during simulation. Table 4 shows the comparison of simulated, ANN, and measured results for resonating frequencies.

Table 4. Comparison of simulated, ANN, and measured results

Resonating Frequency	IE3D Simulated (GHz)	ANN (GHz)	Experimental (GHz)
f_{r1}	1.25	1.253	1.1
f_{r2}	5.25	5.252	5.4
f_{r3}	6.42	6.425	6.4
f_{r4}	8.73	8.734	8.6
f_{r5}	9.86	9.866	9.8



Figure 6. (a) Fabricated 2×4 MSA Array with RP2; (b) Experimental setup for measurement of radiation pattern

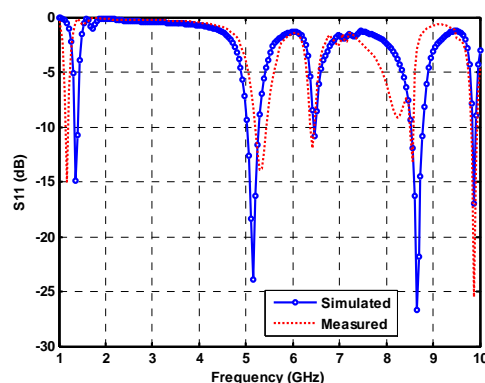


Figure 7. Comparison of simulated and measured reflection coefficient variation for 2×4 MSA array with shorted wall at RP2

Anechoic chamber experimental setup for the measurement of radiation pattern of 2×4 MSA array with a shorted wall at RP2 is shown in Figure 6(b) and the distance between the transmitting and receiving antenna is 200 cm. In this work, E -plane ($E_\theta, \phi = 0^\circ$) is measured in x - z plane and H -plane ($E_\theta, \phi = 90^\circ$) is measured in x - y plane. Comparison plots for simulated and measured radiation patterns at ANN optimized frequencies 1.253, 5.252, 6.425, 8.734, and 9.866 GHz shown in Figures 8(a)-(b)-(c)-(d) and (e) respectively. The 3dB beamwidth is also estimated and summarized in Table 5.

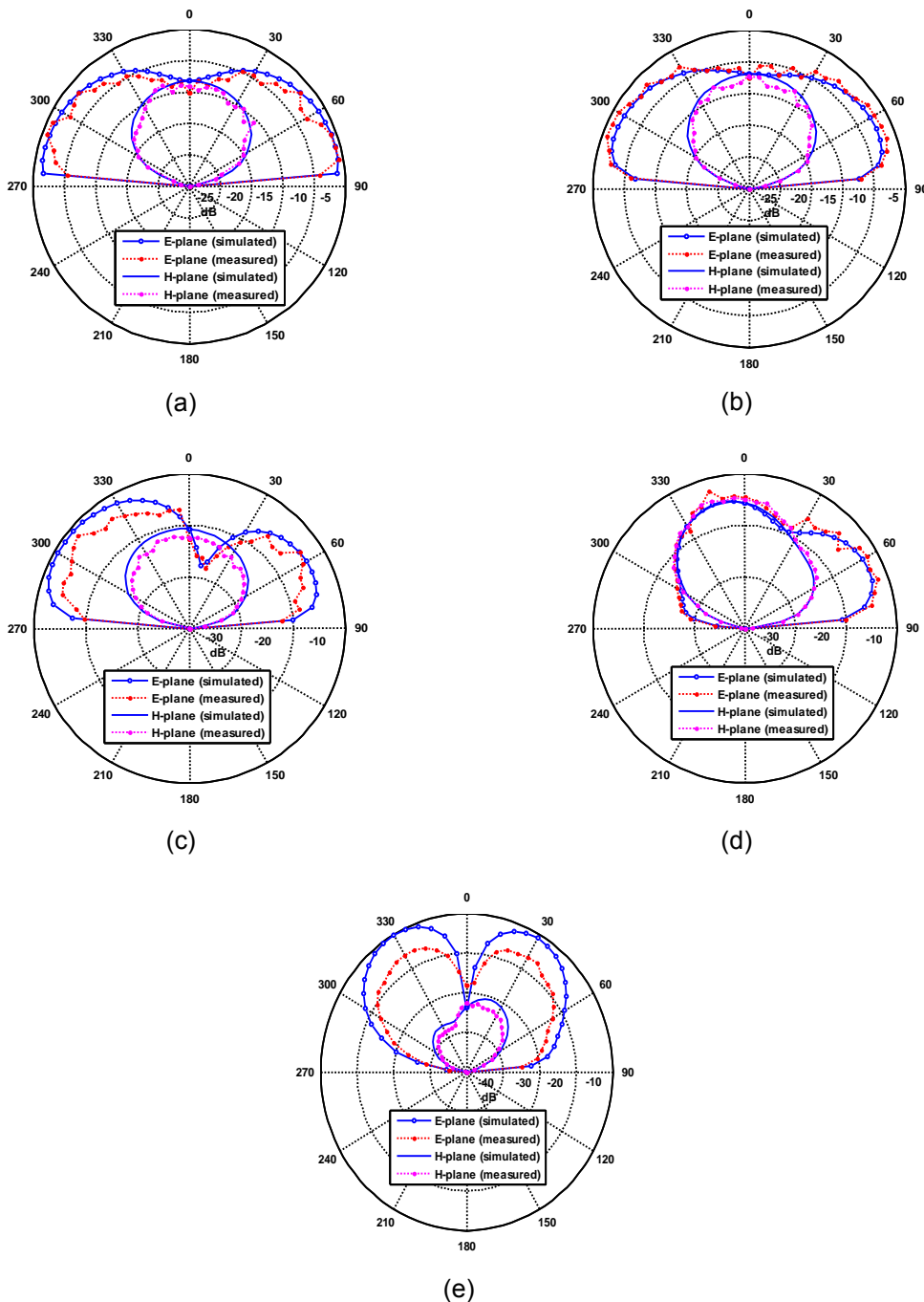


Figure 8. Comparison of simulated and measured radiation pattern at ANN optimized frequencies (a) 1.253 GHz (b) 5.252 GHz (c) 6.425 GHz (d) 8.734 GHz (e) 9.866 GHz

Table 5. Comparison of simulated and measured beamwidths at ANN optimized frequencies

ANN optimized frequency	3dB beamwidth				Angle of Tilt (for E-plane)	Radiation Efficiency (Simulated)
	$E_{\theta}, \phi = 0^{\circ}$ (E-plane)		$E_{\theta}, \phi = 90^{\circ}$ (H-plane)			
	Simulated	Measured	Simulated	Measured		
1.253 GHz	54°	52°	89°	86°	-	81.2 %
5.252 GHz	36°	35°	69°	67°	-	90.5 %
6.425 GHz	62°	59°	93°	90°	30°	73.5 %
8.734 GHz	47°	49°	49°	50°	33°	91.9 %
9.866 GHz	33°	28°	36°	33°	27°	78.0 %

4. Conclusion

In this paper, 32, compact 2×4 MSA array has been designed in simulation media whereas the effect of inserting the shorting wall is carried out with the help of ANN. The developed ANN model predicted the most accurate results for resonant frequencies of the proposed antenna array. A compact 2×4 MSA array has been physically fabricated on a glass epoxy substrate to validate ANN study and results are found quite satisfactory. The proposed antenna array operates at frequencies 1.32, 5.25, 6.42, 8.73, and 9.86 GHz. Its radiation pattern has been measured at ANN optimized frequencies. The fabricated antenna array can be find good applications in L, C, and X band.

References

- [1] Bahl IJ, Bhartia P. *Microstrip Antennas*. Artech House. Dedham, Mass. USA. 1980.
- [2] Nayestanak AAL. W-shaped Enhanced Patch Antenna for Wireless Communication. *Wireless Pers. Commun.* 2007; 43:1257-1265.
- [3] Pandey VK, Vishwakarma BR. Analysis of E-shaped Patch Antenna. *Microwave Opt. Technol. Lett.* 2007; 49:4-7.
- [4] Ansari JA, Dubey SK, Mishra A. Analysis of Half E-shaped Patch for Wideband Application. *Microwave Opt. Technol. Lett.* 2009; 51:1576-1580.
- [5] Deshmukh AA, Kumar G. Compact Broadband S-shaped Microstrip Antennas. *Electronics Lett.* 2006; 42:260-261.
- [6] Meshram MK, Vishwakarma BR. Gap-coupled Microstrip Array Antenna for Wide-Band Operation. *International Journal of Electronics.* 2001; 88(11):1161-1175.
- [7] Wang H, Fang DG, Chen XG. A Compact Single Layer Monopulse Microstrip Antenna Array. *IEEE Trans. on Antennas and Propag.* 2006; 54(2):503-509.
- [8] Svezhentsev AY, Kryzhanovskiy V, Vandenbosch GAE. Cylindrical Microstrip Array Antennas with Slotted Strip-Framed Patches. *Progress in Electromagnetics Research.* 2013; 139:539-558.
- [9] Gujral M, Li JL-W, Yuan T, Qiu C-W. Bandwidth Improvement of Microstrip Antenna Array using Dummy EBG Pattern on Feedline. *Progress in Electromagnetics Research.* 2012; 127: 79-92.
- [10] Qiu L, Zhao F, Xiao K, Chai SL, Mao JJ. Transmit-Receive Isolation Improvement of Antenna Arrays by using EBG Structures. *IEEE Antennas and Wireless Propag. Lett.* 2012; 11:93-96.
- [11] Wang H, Huang XB, Fang DG, Han GB. A Microstrip Antenna Array Formed By Microstrip Line Fed Tooth-Like-Slot Patches. *IEEE Trans. on Antennas and Propag.* 2007; 55(4):1210-1214.
- [12] Liu XF, Jiao YC, Zhang FS, Chen YB. *Design of Conformal Microstrip Antenna Array Mounted on an Irregular Dielectric Surface*. Asia Pacific microwave conference proceedings (AMPC). 2005; Doi: 10.1109/APMC.2005.1606576.
- [13] Seki T, Honma N, Nishikawa K, Tsunekawa K. Millimeter-Wave High-Efficiency Multilayer Parasitic Microstrip Antenna Array on Teflon Substrate. *IEEE Trans. on Microw. Theory and Techniq.* 2005; 53(6):2101-2106.
- [14] Alam MM, Sonchoy MMR, Goni MO. *Design and Performance Analysis of Microstrip Array Antenna*. Progress in Electromagnetics Research Symposium Proceedings. 2009; Moscow, Russia, 1837-1842.
- [15] Alwan EA, Sertel K, Volakis JL. A Simple Equivalent Circuit Model for Ultra Wideband Coupled Arrays. *IEEE Antennas and Wireless Propag. Lett.* 2012; 11:117-120.
- [16] Lin CK, Chung SJ. A Filtering Microstrip Antenna Array. *IEEE Trans. on Microw. Theory and Techniq.* 2011; 59(11):2856-2863.
- [17] Vazquez C, Hotopan G, Hoeye SV, Fernandez M, Herran LF, Heras FL. Microstrip Antenna Design Based on Stacked Patches for Reconfigurable Two Dimensional Planar Array Topologies. *Progress in Electromagnetics Research.* 2009; 97:95-104.
- [18] Patnaik A, Choudhury B, Pradhan P, Mishra RR, Christodoulou C. An ANN Application for Fault Finding in Antenna Arrays. *IEEE Transac. on Antennas and Propag.* 2007; 55(3):775-777.
- [19] Patnaik A, Anagnostou D, Christodoulou CG, Lyke JC. Modeling Frequency Reconfigurable Antenna Array using Neural Networks. *Microwave Opt. Technol. Lett.* 2005; 44(4):351-354.

-
- [20] Dunder O, Uzer D, Gultekin SS, Bayrak M. *Effects of microstrip feed line width on 1×4 rectangular microstrip antenna array electrical parameters and estimation with artificial neural networks*. Progress in Electromagnetic Research Symposium Proceedings. 2012; KL, Malaysia, 1341-1345.
- [21] Wang X, Zhang M, Wang SJ. Practibility Analysis and Application of PBG Structures on Cylindrical Conformal Microstrip Antenna and Array. *Progress in Electromagnetics Research*. 2011; 115:495-507.
- [22] Lee KC. Frequency-Domain Analyses of Nonlinearly Loaded Antenna Arrays using Simulated Annealing Algorithms. *Progress in Electromagnetics Research*. 2005; 53:271-281.
- [23] He QQ, Wang BZ. Design of Microstrip Array Antenna by Using Element Pattern Technique Combining with Taylor Synthesis Method. *Progress in Electromagnetics Research*. 2008; 80:63-76.